

state is the same as that of the "isolated Fe" in the paramagnetic state. This implies that a change occurs in the conduction electron configuration of the "neighboring Fe" across the magnetic transition temperature.

ACKNOWLEDGMENTS

We wish to thank Don Freeman for developing the least squares fitting program, and R. Gutmacher for the x-ray fluorescence analysis.

PHYSICAL REVIEW

VOLUME 162, NUMBER 3

15 OCTOBER 1967

Optical Properties of Vacuum-Evaporated White Tin*

R. A. MACRAE† AND E. T. ARAKAWA

Health Physics Division, Oak Ridge National Laboratory, Oak Ridge, Tennessee

AND

M. W. WILLIAMS‡

Physics Department, University of Tennessee, Knoxville, Tennessee

(Received 5 January 1967; revised manuscript received 19 April 1967)

Near-normal incidence-reflectance data on vacuum-evaporated white tin films, produced *in situ*, are presented for incident photon energies from 2.1 to 14.5 eV. In addition, the real part of the refractive index has been measured from 14.5 to 20.5 eV by the critical-angle method. These results are combined with previously published data for white tin films and an analysis of optical data is carried out from 0.1 to 27.5 eV. Separation of the dielectric constants into contributions due to free and bound electrons indicates interband transitions at 1.2 ± 0.1 and 24.5 ± 0.1 eV, as found by previous workers, and a further interband transition at approximately 3 eV. Tentative identification of these transitions is made using published energy-band calculations. The energy-loss functions for surface and volume plasmons show sharp peaks at 9.2 and 13.4 eV, respectively, in agreement with electron-energy-loss measurements. Sum rules are used to interpret the effective number of electrons per atom at various incident photon energies.

I. INTRODUCTION

THERE is very little data in the literature on the optical constants of white tin¹⁻⁸ and no comprehensive analysis of optical data over an extensive energy range. This paper presents an analysis of the real and imaginary parts, $n(E)$ and $k(E)$, respectively, of the energy-dependent complex refractive index over the energy range 0.1 to 27.5 eV. In order to do this, measurements of optical constants have been made in the energy ranges where insufficient data are available in the literature. The quantities $n(E)$ and $k(E)$ are used

to calculate the real and imaginary parts, $\epsilon_1(E)$ and $\epsilon_2(E)$, respectively, of the complex dielectric constant $\epsilon(E)$ and also the energy-loss functions, $-\text{Im}[1/(\epsilon+1)]$ for surface plasmons and $-\text{Im}(1/\epsilon)$ for volume plasmons. Some discussion and interpretation of these quantities are presented in terms of free-electron-like behavior, interband transitions, and collective oscillations. The interband transitions found in the present analysis are compared with the available band-structure calculations for white tin. In addition, the energy-loss functions are compared with published electron-energy-loss data.

II. SURVEY OF PREVIOUS OPTICAL DATA

Optical constants for tin in the energy range 0.1 to 1.3 eV have been determined by Hodgson² and by Golovashkin and Motulevich.⁴ Both used evaporated tin films which were prepared outside, and then transferred into, the reflectometer. The change in polarization of radiation reflected from these films was analyzed to give $n(E)$ and $k(E)$. There is fair agreement between the values of $n(E)$ and $k(E)$ contained in these two references. However, the data of Golovashkin and Motulevich are more extensive and contain less scatter than that of Hodgson. Lenham and Treherne⁸ have determined $\epsilon_1(E)$ and $\epsilon_2(E)$ for the principal directions in crystalline tin from below 0.1 to 3.1 eV. However, it is found that the values of $n(E)$ and $k(E)$ calculated

* Research sponsored by the U. S. Atomic Energy Commission under contract with Union Carbide Corporation.

† Consultant, Oak Ridge National Laboratory; Jacksonville State University, Jacksonville, Alabama.

‡ Consultant, Oak Ridge National Laboratory.

¹ Landolt-Börnstein, *Zahlenwerte und Funktionen II* (Springer-Verlag, Berlin, 1962) Vol. 8, p. 15.

² J. N. Hodgson, Proc. Phys. Soc. (London) **B68**, 593 (1955).

³ W. C. Walker, O. P. Rustgi, and G. L. Weissler, J. Opt. Soc. Am. **49**, 471 (1959).

⁴ A. I. Golovashkin and G. P. Motulevich, Zh. Eksperim. i Teor. Fiz. **47**, 64 (1964) [English transl.: Soviet Phys.—JETP **20**, 44 (1965)].

⁵ K. Codling, R. P. Madden, W. R. Hunter, and D. W. Angel, J. Opt. Soc. Am. **56**, 189 (1966).

⁶ W. R. Hunter, *Optical Properties and Electronic Structure of Metals and Alloys*, edited by F. Abeles (North-Holland Publishing Company, Amsterdam, 1966), p. 136.

⁷ R. A. MacRae, E. T. Arakawa, and R. N. Hamm, J. Opt. Soc. Am. **56**, A550 (1966).

⁸ A. P. Lenham and D. M. Treherne, J. Opt. Soc. Am. **56**, 752 (1966).

from their $\epsilon_1(E)$ and $\epsilon_2(E)$ do not agree with those for evaporated tin films. In the energy range 1.3 to 14.5 eV there are no recent determinations¹ of $n(E)$ or $k(E)$ for tin films. From 7.5 to 27.5 eV, Walker *et al.*³ have measured the reflectance at 20° angle of incidence from a glass-backed tin film evaporated *in situ*, but the optical constants were not determined from these data. Finally, Hunter⁶ has obtained values of $k(E)$ from 14.5 to 27.5 eV from transmission measurements made on tin films.

III. EXPERIMENTAL PROCEDURE AND EVALUATION OF OPTICAL CONSTANTS

Tin films, produced in the reflectometer, were obtained by evaporating tin of 99.999% purity from a small aperture in a Ta boat onto a quartz slide. The tin was raised to its melting point in about 20 sec and evaporated at about 1 000 Å/sec to produce a film approximately 2 500 Å thick. A pressure of 10^{-6} Torr was maintained in the apparatus. To check the quality of the vacuum-Sn surface used for reflectance measurements, the reflectances from both the vacuum-Sn and quartz-Sn surfaces were measured at a wavelength of 2 500 Å in the region of quartz transmission. The quartz-Sn surface has less chance of contamination than the vacuum-Sn surface and always appears shiny in the visible region even if the other surface is of poor quality. The data reported here were obtained on a tin film for which the reflectance from the quartz-Sn surface, corrected for the quartz transmission and reflection, was equal to the reflectance of the vacuum-Sn surface. This indicates a good vacuum-Sn surface. When formed and maintained at a pressure of 10^{-6} Torr, the transmittance of the tin film in the visible region

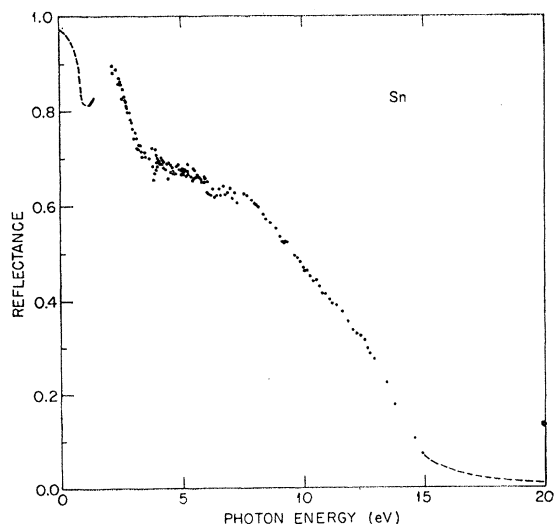


FIG. 1. Reflectance of Sn films as a function of incident photon energy. The curve is a composite of data obtained for the present analysis and that of Refs. 4 and 6. Circles represent experimental reflectance at 15° angle of incidence; dashed lines indicate normal-incidence reflectance calculated from n and k .

was less than 0.01%, as compared with a neutral density filter. After exposure to the atmosphere, slight deterioration of the film was noted; the transmittance increasing to about 0.1% in the visible. The apparatus used for reflectance and critical angle measurements has been described elsewhere.^{9,10}

For incident photon energies from 2.1 to 14.5 eV, reflectance measurements were made at an angle of incidence of 15°. From 14.5 to 20.5 eV, where $n(E) < 1$ and $k(E) \approx 0$, $n(E)$ was determined by the critical-angle method.¹¹ These values of $n(E)$ were then combined with Hunter's⁶ values of $k(E)$, from transmission measurements in this energy range, to yield the normal-incidence reflectance as a function of incident-photon energy. These values are plotted in Fig. 1. Also plotted in Fig. 1 is the normal-incidence reflectance in the energy range 0.1 to 1.3 eV obtained from Golovashkin and Motulevich's⁴ $n(E)$ and $k(E)$.

A Kramers-Kronig (KK) analysis¹² was performed on the complete reflectance data presented in Fig. 1 to yield $n(E)$ and $k(E)$ over the energy range 2.1 to 14.5 eV. The usual method¹³ employing extrapolation of reflectance to higher energies was not used. Since values of $n(E)$ and $k(E)$ were already known in the energy ranges 0.1 to 1.3 eV and 14.5 to 20.5 eV, the phase change on reflection $\theta(E)$ could be calculated in these regions from Eq. (1)

$$\theta(E) = \tan^{-1} 2k / (1 - n^2 - k^2). \quad (1)$$

This relation is obtained from Fresnel's equations assuming the complex refractive index in the form $(n - ik)$ and the complex reflectance amplitude $\tilde{r} = re^{i\theta}$, where the reflectance R equals $|\tilde{r}|^2$. θ is restricted to $-\pi \leq \theta \leq 0$. The phase change is also given by Eq. (2)

$$\begin{aligned} \theta(E) &= -\frac{E}{\pi} \int_0^{\infty} \frac{\ln R(E')}{(E')^2 - E^2} dE' \\ &= -\frac{E}{\pi} \int_0^{20.5 \text{ eV}} \frac{\ln R(E')}{(E')^2 - E^2} dE' \\ &\quad + \frac{E}{\pi} \int_{20.5 \text{ eV}}^{\infty} \frac{\ln R(E') dE'}{(E')^2 - E^2}. \quad (2) \end{aligned}$$

The integral from 0 to 20.5 eV in this equation can be calculated from the known reflectance presented in Fig. 1; hence, where $\theta(E)$ is known, the integral from 20.5 eV to infinite energy can be calculated. Values of this second integral, calculated in this way, have been

⁹ R. H. Huebner, E. T. Arakawa, R. A. MacRae, and R. N. Hamm, *J. Opt. Soc. Am.* **54**, 1434 (1964).

¹⁰ T. M. Jelinek, R. N. Hamm, E. T. Arakawa, and R. H. Huebner, *J. Opt. Soc. Am.* **56**, 185 (1966).

¹¹ W. R. Hunter, *J. Phys. Radium* **25**, 154 (1964).

¹² See, e.g., F. C. Jahoda, *Phys. Rev.* **107**, 1261 (1957); F. Stern, *Solid State Physics*, edited by F. Seitz and D. Turnbull (Academic Press Inc., New York, 1963), Vol. 15, p. 299.

¹³ See, e.g., H. Ehrenreich, H. R. Philipp, and B. Segall, *Phys. Rev.* **132**, 1918 (1963).

plotted as $\Delta\theta$ in Fig. 2. $\Delta\theta$ is the contribution to the phase change on reflection due to absorption in the energy region above 20.5 eV. $\Delta\theta$ was interpolated in the energy range 1.3 to 14.5 eV by a smoothly varying function as shown by the curve in Fig. 2. By substitution back into Eq. (2), $\theta(E)$ was then obtained in the energy range 2.1 to 14.5 eV. A knowledge of $\theta(E)$ and $R(E)$ in the interpolated region then yielded $n(E)$ and $k(E)$ from

$$n = (1 - r^2) / (1 + r^2 - 2r \cos\theta)$$

and

$$k = (-2r \sin\theta) / (1 + r^2 - 2r \cos\theta).$$

Since Hunter⁶ had measured $k(E)$ up to 27.5 eV, values of $n(E)$ up to 27.5 eV were estimated by making a smooth extrapolation through the points $n=0.88$ at 20.5 eV and $n=0.965$ at 27.5 eV.

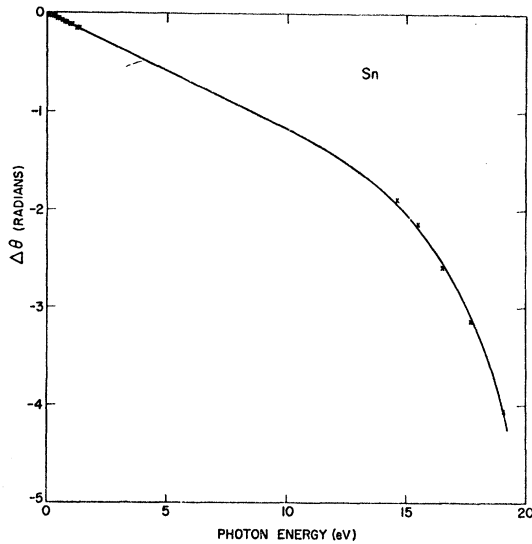


FIG. 2. Contribution to the phase angle due to absorption above 20.5 eV as a function of incident photon energy. (X-calculated values).

Values of $n(E)$ and $k(E)$ over the energy range 0.1 to 27.5 eV are shown in Fig. 3, and the dielectric constants, $\epsilon_1(E)$ and $\epsilon_2(E)$, are shown in Fig. 4 over the energy range of interest in the interpretation of the energy-loss functions.

IV. ANALYSIS AND DISCUSSION

It has been shown¹⁴ that the complex dielectric constant of a metal can be written as

$$\epsilon(E) = \epsilon^{(f)}(E) + \delta\epsilon^{(b)}(E), \quad (3)$$

where $\epsilon^{(f)}(E)$ is the contribution due to free electrons and $\delta\epsilon^{(b)}(E)$ is that due to bound electrons.

From the free-electron theory,¹⁵ we can express

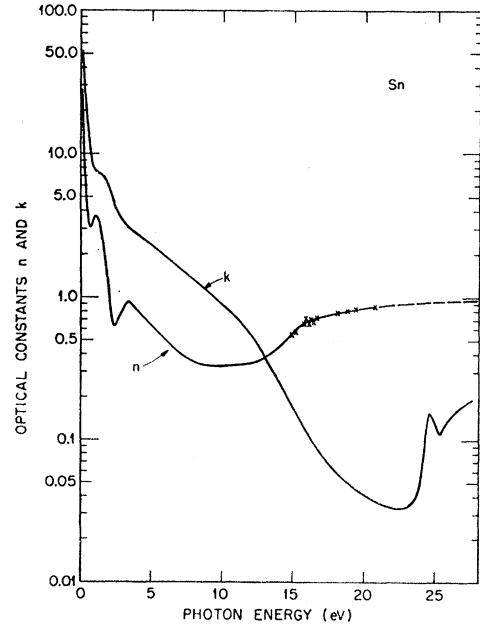


FIG. 3. Optical constants of Sn as a function of incident photon energy. The curve is a composite of data obtained from the present analysis and from Refs. 4 and 6. (X-critical-angle method.)

$\epsilon^{(f)}(E)$ in the following form:

$$\epsilon^{(f)}(E) = 1 - E_{pa}^2 / E(E + i\hbar/\tau), \quad (4)$$

where $E_{pa} = \hbar(4\pi N n_{\text{eff}} e^2 / m_{\text{eff}})^{1/2}$, τ is the relaxation time, N is the number of atoms per unit volume of the

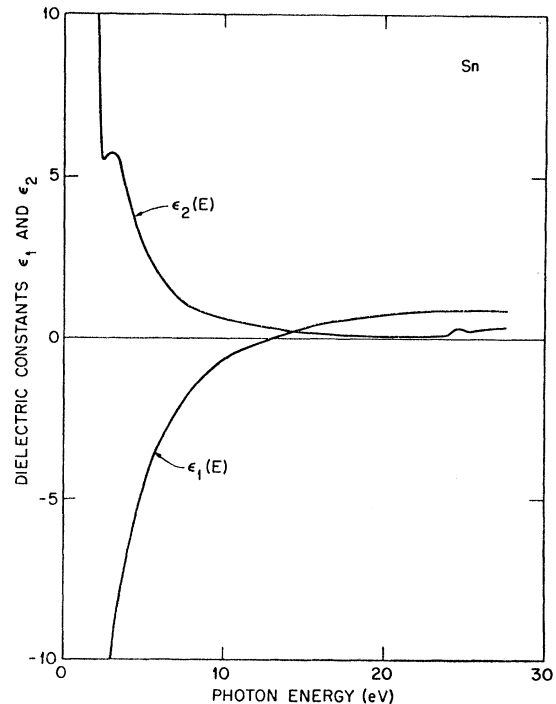


FIG. 4. Dielectric constants of Sn as a function of incident photon energy.

¹⁴ H. Ehrenreich and H. R. Philipp, Phys. Rev. **128**, 1622 (1962).

¹⁵ See, e.g., L. G. Schulz, Phil. Mag. Suppl. **6**, 102 (1957).

crystal, m_{eff} is the effective mass of the electrons, and n_{eff} is the effective number of electrons per atom contributing to the optical properties at energies below the threshold for transitions between electronic bands.

The free-electron theory has been modified by Dingle¹⁶ and by Holstein¹⁷ to allow for the anomalous skin effect.^{15,18} However, this effect is found to be very small in tin at room temperature⁴ and no allowance is made for it in this analysis.

X-ray studies show that tin has two $5p$ electrons in the valence band and two $5s$ electrons in a (overlapping) band at approximately 1.4 eV. The next lowest bands are $4d$ bands at 23.9 and 24.4 eV.¹⁹ In tin, the unique separation of the complex dielectric constant into free-electron and bound-electron contributions is difficult because of the low energy associated with the first interband transition. The x-ray studies indicate that the contribution to the imaginary part of the dielectric constant due to bound electrons should go through a maximum at approximately 1.4 eV. This interband transition may cause the dielectric constant to deviate from the free-electron formula down to the lowest energy at which measurements were made. Thus, in tin, there is no extended energy region over which it is known that the behavior of the dielectric constant should be "free-electron-like" and the data cannot be analyzed to yield a unique dependence of the relaxation time on energy. In order to make a reasonable separation of the measured dielectric constant into free-electron and bound-electron contributions, we have assumed that interband transitions have no influence at the lowest energy at which measurements were made and the relaxation time is energy-independent. Then the following equations:

$$\begin{aligned} \epsilon_1(\text{exp}) &= \epsilon_1^{(f)}(E) + \delta\epsilon_1^{(b)}(E) \\ &= 1 - [E_{pa}^2 / (E^2 + (\hbar/\tau)^2)] + \delta\epsilon_1^{(b)}(E), \quad (5) \end{aligned}$$

$$\begin{aligned} \epsilon_2(\text{exp}) &= \epsilon_2^{(f)}(E) + \delta\epsilon_2^{(b)}(E) \\ &= \frac{\hbar}{\tau E} [E_{pa}^2 / (E^2 + (\hbar/\tau)^2)] + \delta\epsilon_2^{(b)}(E), \quad (6) \end{aligned}$$

for the experimental values of ϵ_1 and ϵ_2 yield $E_{pa} = 8.16$ eV and $\tau = 4.20 \times 10^{-13}$ sec, with $\delta\epsilon_1^{(b)}(E) = \delta\epsilon_2^{(b)}(E) = 0$ at 0.1 eV. With m_{eff} taken equal to the free-electron mass and for a density of 7.3 g/cm³, $E_{pa} = 8.16$ eV gives a value of 1.30 for n_{eff} . For comparison Hodgson² obtained 1.33, and Chambers²⁰ 1.1 from observations of the anomalous skin effect. Measurements such as electrical conductivity also indicate that n_{eff} is much

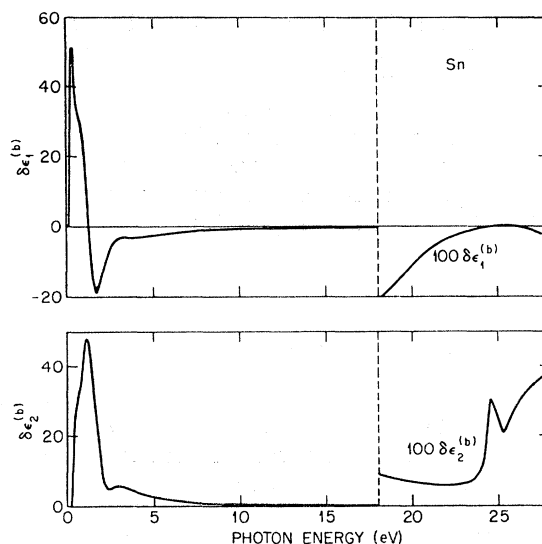


FIG. 5. Contributions to ϵ_1 and ϵ_2 due to bound electrons, $\delta\epsilon_1^{(b)}$ and $\delta\epsilon_2^{(b)}$, respectively, as a function of incident photon energy.

less than four, the number of valence electrons per atom usually assumed for tin. This indicates the existence of a "Jones" zone which contains about four states per atom.²¹ In fact, in multivalent metals, such as tin, where the free electrons occupy several overlapping energy bands, n_{eff} and m_{eff} are regarded as representing averages of the numbers of electrons and the effective masses of the electrons in the various bands.

In order to show the energies of interband transitions, $\delta\epsilon_1^{(b)}(E)$ and $\delta\epsilon_2^{(b)}(E)$, calculated from Eqs. (5) and (6) with $E_{pa} = 8.16$ eV, $\tau = 4.20 \times 10^{-13}$ sec, and the experimental values of ϵ_1 and ϵ_2 , are plotted as a function of energy in Fig. 5. It is seen that there is a well-defined interband transition^{22,23} identified by a zero in $\delta\epsilon_1^{(b)}(E)$ and a maximum in $\delta\epsilon_2^{(b)}(E)$ at (1.2 ± 0.1) eV. This interband transition which corresponds to the O_{II} x-ray level was obtained by Golovashkin and Motulevich⁴ from the maximum slope of a plot of $k(E)/\lambda(E)$ versus the energy of the photons, where λ is the wavelength. Hodgson² did not find this transition; instead, he obtains a constant n_{eff} over the energy range 0.1 to 1.3 eV and attributes deviations of $\epsilon_2(E)$ from the free-electron formula to a dependence of τ on E .

At higher energies the structure in $\delta\epsilon_1^{(b)}(E)$ and $\delta\epsilon_2^{(b)}(E)$ is more complicated since more than one interband transition contributes to the calculated values of the real and imaginary parts of the dielectric constant. The most recent measurements of the transmittance of tin films⁵ locate the N_{IV} and N_V x-ray edges at 24.9 ± 0.1 eV and 23.8 ± 0.1 eV, respectively. These

¹⁶ R. B. Dingle, *Physica* **19**, 311, 348, 729, 1187 (1953).

¹⁷ T. Holstein, *Phys. Rev.* **88**, 1425 (1952); **96**, 535 (1954).

¹⁸ G. E. H. Reuter and E. H. Sondheimer, *Proc. Roy. Soc. (London)* **A195**, 336 (1948).

¹⁹ A. E. Sandström, in *Handbuch der Physik*, edited by S. Flügge (Springer-Verlag, Berlin, 1957), Vol. 30, p. 226.

²⁰ R. B. Chambers, *Proc. Roy. Soc. (London)* **A215**, 481 (1952).

²¹ N. F. Mott and H. Jones, *The Theory of the Properties of Metals and Alloys* (Dover Publications, Inc., New York, 1958).

²² H. Ehrenreich, *IEEE Spectrum* **2**, 162 (1965).

²³ H. Raether, in *Springer Tracts in Modern Physics*, edited by G. Höhler, S. Flügge, F. Hund, and E. A. Niekisch (Springer-Verlag, Inc., New York, 1965), Vol. 38, p. 84.

4d to 5p electron transitions are unresolved in Fig. 5 at 24.5 ± 0.1 eV since the values of $k(E)$ obtained by Hunter from transmission measurements in this energy region do not resolve the two transitions. The variation of $\delta\epsilon_2^{(b)}(E)$ in Fig. 5 also indicates the possibility of a weak interband transition at about 3 eV.

It is to be noted that, ideally, the KK relation²⁴ between $\delta\epsilon_1^{(b)}(E)$ and $\delta\epsilon_2^{(b)}(E)$ should be obeyed at all energies. The calculated free-electron components $\epsilon_1^{(f)}(E)$ and $\epsilon_2^{(f)}(E)$ must obey the KK relation and the experimental values of $\epsilon_1(E)$ and $\epsilon_2(E)$, over most of the energy range, were obtained from a KK analysis. Thus the components $\delta\epsilon_1^{(b)}(E)$ and $\delta\epsilon_2^{(b)}(E)$ obtained from Eq. (3) and presented in Fig. 5 should obey the KK relation. Reasonable agreement was obtained between $\delta\epsilon_1^{(b)}(E)$ calculated from Eq. (3) and from $\delta\epsilon_2^{(b)}(E)$ using the KK relation for energies above 0.5 eV. The agreement was not as good at the lower energies, the difference becoming increasingly larger as $E \rightarrow 0$ because of our method of analysis, in which $\delta\epsilon_1^{(b)}(E) = \delta\epsilon_2^{(b)}(E) = 0$ from 0 to 0.1 eV.

Weisz²⁵ has calculated the band structure for white tin without spin-orbit effects and then found spin-orbit corrections to this band structure at a few symmetry points in the Brillouin zone. Of the allowed direct transitions, $V_4 \rightarrow V_3$ at 2.0 eV is the closest in energy to our observed interband transition at 1.2 eV. Furthermore on the basis of phase-space arguments, this transition has a relatively high probability. The observed 3-eV transition could be one of several possible direct transitions in the region of 3 eV at the point W or the transition $\Gamma_5^+ \rightarrow \Gamma_4^-$ at 3.9 eV. Although $V_2 \rightarrow V_3$ at 3.0 eV has a value comparable with possible transitions at the point W and with the observed value, this transition and the transition $V_1 \rightarrow V_3$ at 3.7 eV both have lower probabilities on the basis of phase-space arguments.

The energy-loss functions $-\text{Im}(1/\epsilon)$ and $-\text{Im}[1/(\epsilon+1)]$ for volume and surface plasmons,²⁶ respectively, were calculated from the experimentally-determined values of $\epsilon_1(E)$ and $\epsilon_2(E)$ and are plotted versus photon energy in Fig. 6. These functions describe the probability that fast electrons traversing the material will lose energy due to induced volume- and surface-collective electron oscillations, respectively. Ritchie predicts that the surface (or lowered) plasma loss should occur at $\frac{1}{2}\sqrt{2}E_p$ for a planar film, where E_p is the observed volume-plasma energy.

In Fig. 6 the $-\text{Im}(1/\epsilon)$ function shows a sharp maximum at 13.4 eV, and the $-\text{Im}[1/(\epsilon+1)]$ function a sharp maximum at 9.2 eV. The sharpness of these maxima indicates that both energy losses should be observed when fast electrons traverse tin films. Characteristic-electron-energy losses have been ob-

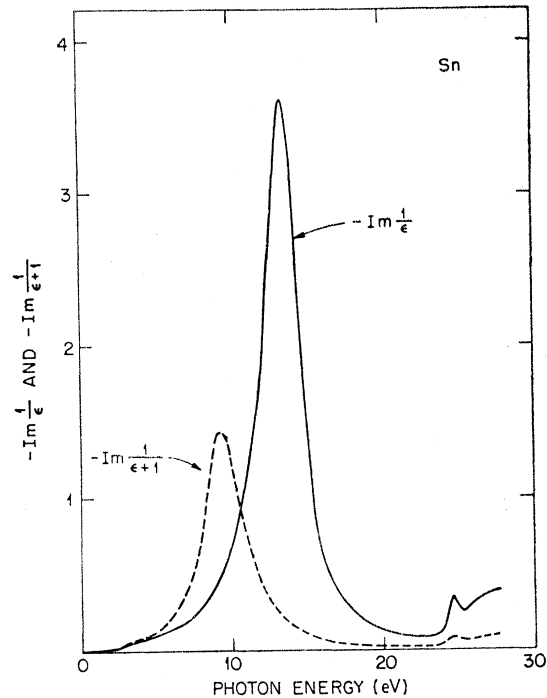


FIG. 6. Energy-loss functions, $-\text{Im}[1/(\epsilon+1)]$ for surface plasmons and $-\text{Im}(1/\epsilon)$ for volume plasmons, of Sn as a function of incident photon energy.

served in tin by Powell²⁷ at 14.1 and 10.4 eV, with surface oxidation causing the replacement of the 10.4 eV-low-lying loss by a modified low-lying loss at 8.3 ± 0.2 eV. The agreement of the maximum of the volume-plasma-loss function at 13.4 eV with the 14.1 eV electron-energy loss observed by Powell is satisfactory. Furthermore, the optical data unambiguously identify this electron-energy loss as due to induced volume-electron plasma oscillations, since in this energy region ϵ_1 goes through zero and ϵ_2 is small and shows no structure²⁸ (Fig. 4). If the loss were due to an induced interband transition there would be a relative maximum in ϵ_2 . E_p was also observed in tin by Walker *et al.*³ at 13.6 eV from the onset of optical transmission. The maximum of the surface-plasma-loss function at 9.2 eV is seen to agree with the low-lying loss observed by Powell. This is identified as a surface-plasma loss, for the same reasons as the volume-plasma loss, since ϵ_1 passes through -1 and ϵ_2 shows no structure in this region.

The observed volume-plasma energy E_p is displaced from $E_{pa} = 8.16$ eV to $E_p = 13.4$ eV because of the negative value of $\delta\epsilon_1^{(b)}(E)$ in this energy range²³ (Fig. 5). In general, interband transitions at energies below E_{pa} increase the value of E_p while interband transitions above E_{pa} decrease E_p . In tin, the 1.2-eV

²⁴ E. A. Taft and H. R. Philipp, Phys. Rev. **138**, A197 (1965).

²⁵ G. Weisz, Phys. Rev. **149**, 504 (1966).

²⁶ R. H. Ritchie, Phys. Rev. **106**, 874 (1957).

²⁷ C. J. Powell, Proc. Phys. Soc. (London) **A76**, 593 (1960).

²⁸ H. Fröhlich and H. Pelzer, Proc. Phys. Soc. (London) **A68**, 525 (1955).

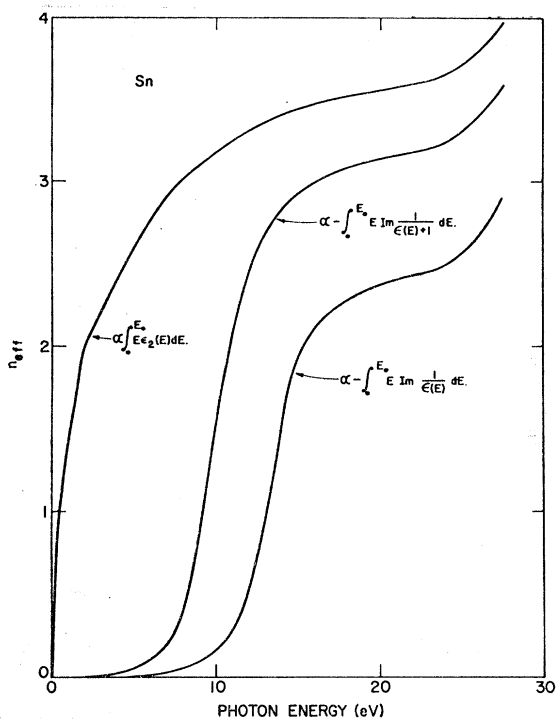


FIG. 7. The effective number of electrons per atom n_{eff} as a function of incident photon energy from numerical integrations of $E\epsilon_2(E)$, $-E \text{Im}[1/(\epsilon(E)+1)]$ and $-E \text{Im}[1/\epsilon(E)]$.

transition is the most effective in this respect, and the net result is an increase in the observed volume plasma energy. Another way of looking at this is to say that at higher incident photon energies, a greater number of electrons per unit volume are free to participate in collective oscillations.

Use of the sum rules^{13,29}

$$\int_0^{E_0} E\epsilon_2(E)dE = \frac{1}{2}\pi\hbar^2 \left(\frac{4\pi N n_{\text{eff}}(E_0) e^2}{m_{\text{eff}}} \right) \quad (7)$$

and

$$-\int_0^{E_0} E \text{Im} \frac{1}{\epsilon(E)} dE = \frac{1}{2}\pi\hbar^2 \left(\frac{4\pi N n_{\text{eff}}(E_0) e^2}{m_{\text{eff}}} \right), \quad (8)$$

illustrates the meaning of n_{eff} . Equation (7) can be used to calculate $n_{\text{eff}}(E_0)$, which is the effective number of electrons per atom contributing to the optical transitions in the energy range up to E_0 . In the energy range 0 to 0.1 eV, where no experimental data were available, $E\epsilon_2^{(c)}(E)$ was calculated from Eq. (6) assuming $E_{pa} = 8.16$ eV, $\tau = 4.20 \times 10^{-15}$ sec and $\delta\epsilon_2^{(b)}(E) = 0$. Then n_{eff} was calculated from Eq. (7) assuming m_{eff} to be the free-electron mass. This n_{eff} is plotted against E_0 in Fig. 7. The initial rapid rise in n_{eff} is due to free-electron effects which, in the absence of interband transitions, would produce saturation at a value of

$n_{\text{eff}} = 1.3$.²⁴ The continued rise of n_{eff} above 1.3 is due to the interband transitions at 1.2 and 3 eV. By $E_0 = 24$ eV, n_{eff} is approaching saturation and the further sharp rise above 24 eV is due to the interband transition at 24.5 eV. Our calculation of $E\epsilon_2(E)$ as E approaches zero yields an optical conductivity $\{\sigma = E\epsilon_2/2\hbar\}$ of $5.7 \times 10^4 \Omega^{-1} \text{cm}^{-1}$. This can be compared with the measured dc values for bulk tin of 7×10^4 to $9 \times 10^4 \Omega^{-1} \text{cm}^{-1}$ at 20°C.³⁰ The agreement is considered satisfactory in view of the uncertainty in the dc value; in fact, it is reasonable that the conductivity of tin in the form of a thin film should be less than that for bulk tin.

Equation (8), which is the sum rule for the energy-loss function for volume plasmons, yields a value for n_{eff} which is the effective number of electrons per atom taking part in volume-plasma oscillations. This n_{eff} is also plotted in Fig. 7 and, as expected, does not begin to rise sharply until the energy-loss function $-\text{Im}[1/\epsilon(E)]$ rises sharply.

A sum rule can be written for the energy-loss function for surface plasmons which takes the form³¹

$$-\int_0^{E_0} E \text{Im} \left(\frac{1}{\epsilon(E)+1} \right) dE = \frac{1}{8}\pi\hbar^2 \left(\frac{4\pi N n_{\text{eff}}(E_0) e^2}{m_{\text{eff}}} \right). \quad (9)$$

Using Eq. (9) one obtains an $n_{\text{eff}}(E_0)$ which is the effective number of electrons per atom participating in surface-plasma oscillations. This $n_{\text{eff}}(E_0)$ is also shown in Fig. 7 and it is seen that it begins to rise sharply when the energy loss function $-\text{Im}[1/(\epsilon(E)+1)]$ rises sharply.

All the sum rules should yield the same n_{eff} at high enough energies. The values obtained for n_{eff} from the different sum rules provides an estimation of the relative accuracy of the experimental values of $\epsilon_2(E)$ over various energy ranges. The values obtained from $\int_0^{E_0} E\epsilon_2(E)dE$ over the whole energy range depend mainly on the values of $\epsilon_2(E)$ in the low-energy region, below the threshold for interband transitions. On the other hand, the values of n_{eff} obtained from $-\int_0^{E_0} E \times \text{Im}[1/(\epsilon(E)+1)]dE$ depend mainly on the value of ϵ_2 , where $\epsilon_1 = -1$, i.e., at 9.2 eV, the surface-plasma resonance energy, and the values obtained from $-\int_0^{E_0} E \text{Im}[1/\epsilon(E)]dE$ depend mainly on the value of ϵ_2 , where $\epsilon_1 = 0$; i.e., at 13.4 eV, the volume-plasma resonance energy. Thus an examination of Fig. 7 shows that the experimental values of $\epsilon_2(E)$ in the regions of 9 and 13 eV must be too high compared with the values at lower energies.

ACKNOWLEDGMENT

The authors wish to acknowledge stimulating discussions with Dr. R. H. Ritchie and Dr. H. C. Schweinler.

²⁹ See, e.g., P. Nozières and D. Pines, Phys. Rev. **113**, 1254 (1959).

³⁰ Handbook of Chemistry and Physics (Chemical Rubber Company, Cleveland, 1959), 41st ed., p. 2595.

³¹ R. H. Ritchie (private communication).